Enhanced carrier injection in Schottky contacts using dopant segregation: a Monte Carlo research

2009 Semicond. Sci. Technol. 24 025022

(http://iopscience.iop.org/0268-1242/24/2/025022)

Semicond. Sci. Technol. **24** (2009) 025022 (6pp) doi:10.1088/0268-1242/24/2/025022

Enhanced carrier injection in Schottky contacts using dopant segregation: a Monte Carlo research

Elena Pascual[1], María J Martín[1], Raúl Rengel[1], Guilhem Larrieu[2] and Emmanuel Dubois[2]

[1] Departamento de Física Aplicada, Universidad de Salamanca, 37008 Salamanca, Spain
[2] Institut d'Electronique de Microélectronique et de Nanotechnologie, IEMN/ISEN UMR CNRS 8520, 59652 Villeneuve d'Ascq Cedex, France

E-mail: elenapc@usal.es

Received 11 June 2008, in final form 18 November 2008
Published 20 January 2009
Online at stacks.iop.org/SST/24/025022

Abstract
In this paper we present a Monte Carlo research of the impact, on carrier transport, of including a dopant-segregated layer adjacent to the Schottky contact in back-to-back diodes. A comparison with a homogeneous structure is developed, evidencing that the doped layer boosts the tunneling current through the Schottky barrier, thus significantly improving the injection of carriers at the contact. We have carried out a complete study of carrier injection and transport in the region close to the reverse-biased contact together with the analysis of internal quantities such as conduction band, carrier density and electric field. The effect of temperature on the current is also evaluated. The study of the velocity distribution functions and the average number of scatterings undergone by the carriers reveals that devices with dopant segregation exhibit an enhancement of the ballistic transport in the first nanometers close to the Schottky contact.

1. Introduction

The performance problems found in the scaling process of silicon MOSFETs over the last years are imposing the exploration of new architecture options, as has been pointed out in the International Technology Roadmap for Semiconductors [1]. One of the different alternatives to conventional devices is the Schottky barrier (SB)-MOSFET, where the doped source and drain regions are replaced by Schottky contacts, allowing improved scalability and reduced short channel effects [2]. Moreover, a lower thermal budget is necessary in their fabrication process since no high temperature spike or flash anneals are required to activate S/D dopants, which is desirable for the integration with other solutions such as strained Si or SiGe channels [3]. In SB-MOSFETs, the injection of carriers across the source contact is a key issue to achieve high drive-current values in the on state. Recent publications have pointed out the need of barrier heights at the source Schottky junction lower than 0.10 eV in order to compete with highly doped S/D MOSFETs, because the drive current is significantly lowered for higher Schottky barriers [4, 5]. In the case of SB p-type MOSFETs, platinum silicide (PtSi) is the most commonly used, presenting a barrier height to holes around 0.22 eV [6]. For n-type devices, the lowest Schottky barriers are obtained using rare earth silicides based on erbium (of 0.28 eV, see [7]) or ytterbium (of 0.27 eV, see [8]). In order to achieve lower effective values of the Schottky barrier height, the dopant-segregation (DS) technique has been proposed [9, 10]. The basic idea relies on the incorporation of a highly doped layer at the Schottky interface, thus modifying the potential profile inside the semiconductor with the aim of favoring the injection of carriers.

From an experimental point of view, this is not a simple task; several fabrication procedures can be used to achieve the integration of the dopant layer [10, 11]. In a first flavor, a shallow implantation into Si is followed by metal deposition and silicidation annealing. According to this first scheme, the implantation energy must be finely tuned to confine most of the dopants over a superficial silicon layer that will be totally consumed by the silicidation reaction. Dopant pile-up is expected to take place at the silicide/silicon interface because

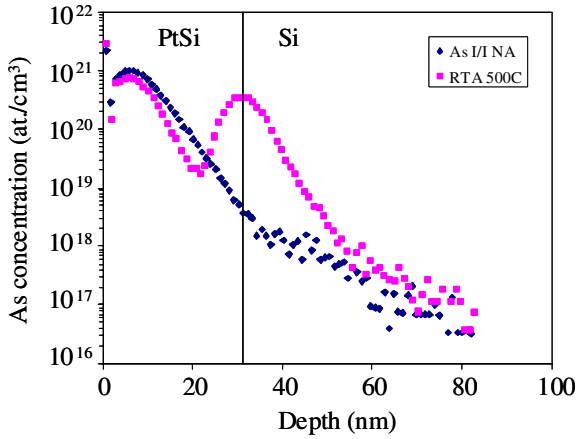

Figure 1. Arsenic concentration profiles obtained by secondary ion mass spectroscopy (SIMS) as implanted in a 32 nm thick PtSi overlayer (diamond symbols) and after a 500 °C post-implantation anneal (square symbols). The sharp As (donor) pile-up evidenced at the PtSi/Si interface is expected to induce the localized band bending shown in figure 2(*b*).

(This figure is in colour only in the electronic version)

of the limited solubility of dopants into the silicide phase. In a second flavor, implantation-to-metal (ITM) can be used to avoid implantation into silicon, thus avoiding problems related to channeling and defect generation. Dopant segregation also takes place due to the silicidation thermal budget. Finally, implantation-to-silicide (ITS) constitutes a third solution for which dopant pile-up must be initiated by a low temperature post-silicidation activation step.

The advantage associated with the last techniques is to confine dopants in the silicide layer without the generation of defects, thus enhancing the segregation effect governed by solid solubility and diffusion mechanisms. As far as p-MOSFETs are considered, Schottky source/drain have been integrated based on a low barrier silicide (PtSi) coupled to boron (B) segregation, yielding a 50% improvement on the current drive [10]. Alternatively, n-type impurities can be introduced to produce an inverse band bending at the Schottky junction that favors electron injection. Following this strategy, As^+ has been implanted at 25 keV with a dose of 10^{15} cm^{-2} in an already formed 30 nm thick PtSi layer. Figure 1 shows the resulting chemical As concentration profiles obtained by secondary ion mass spectrometry (SIMS) for both the as-implanted and final profiles after a post-silicidation annealing step at 500 °C for 5 min. Similar to the case of B segregation, a sharp pile-up of As is observed at the PtSi/Si interface. This system is relevant to the case under study that considers the injection and transport of electrons.

Other authors have also evidenced an important increase of current in Schottky contacts with dopant segregation through the study of *I–V* characteristics [12–14]. However, the effects of a thin layer of dopants adjacent to the contact have not been investigated from a microscopic point of view, so accurate modeling of electronic transport is required. The most important processes involved are thermionic and tunneling injection (from metal to semiconductor) and thermionic and tunneling absorption (from semiconductor to metal) [15]. In particular, the quantum tunneling injection current can be of great importance in the reverse bias regime, so it must be carefully considered.

In this work, we present a Monte Carlo (MC) device simulation of carrier transport in Schottky contacts including the effect of dopant-segregated layers, with a special stress on non-equilibrium phenomena and ballisticity. In the MC method, the microscopic nature of electronic charge transport is reproduced thus providing an exact solution of the Boltzmann transport equation. Moreover, it is possible to obtain valuable information about the character of transport and non-equilibrium effects by means of the study of internal quantities such as concentration, energy, electric field profiles, time average velocity distribution functions, scattering mechanisms, etc. The paper is structured as follows: in section 2 we briefly describe our model and the main features of the simulated structures. Section 3 shows the effect of the inclusion of a DS layer in a back-to-back diode as compared to a homogeneous structure with particular attention to the analysis of internal quantities. A thorough study of transport inside the device and the existence of quasi-ballistic effects is provided. Finally, the main conclusions are detailed in section 4.

2. Simulated structure and Monte Carlo procedure

The simulated structures consist of back-to-back Schottky diodes with a low doped silicon substrate that already present a relatively low Schottky barrier to electrons. This kind of structure reproduces the lateral configuration of the source/drain contacts of a MOSFET with the advantage of suppressing parasitic resistance effects; moreover, back-to-back diodes are particularly adequate to experimentally characterize the properties of the Schottky barrier, a highly relevant issue from the experimental point of view [6]. Figure 2(*a*) shows a schematic of the band profile of a Schottky junction at equilibrium, where transport essentially takes place through thermionic emission. Our objective is to further promote electron injection by tunneling. For that purpose, the dopant-segregation effect is accounted for by considering a thin layer of activated donors; the inclusion of the dopant layer induces a band bending in the region close to the Schottky junction, thus yielding a thinner tunneling path for the electrons from the metal to the semiconductor (the new band profile at equilibrium as shown in figure 2(*b*)).

The structure can be represented by the series combination of lumped elements as schematized in figure 3 [6]. When bias is applied, the total current is controlled by the current provided by the corresponding reverse-biased Schottky contact. We have simulated a conventional back-to-back structure (with no dopant-segregated layer, from now on, NDS1) and the same one with a dopant-segregated layer of 20 nm—with doping equal to 10^{18} cm^{-3}—assuming that dopants are activated in silicon at close proximity of the interface (from now on, the DS structure). Although figure 1 shows that the concentration of segregated As dopants can peak above 10^{20} cm^{-3}, it should be kept in mind that SIMS analysis provides chemical information but does not reveal the state of activation of dopants. Actually,

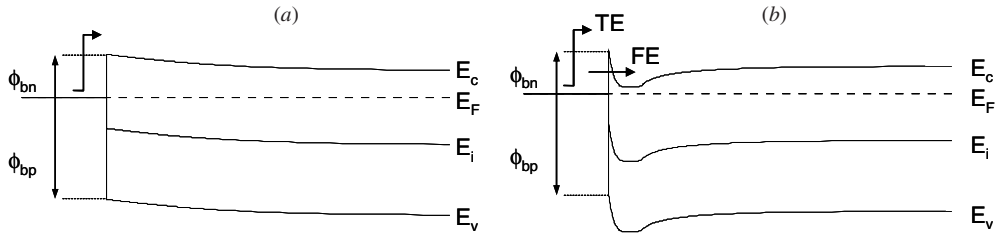

Figure 2. Band structure at equilibrium of a Schottky contact on a substrate featuring a low n-type base concentration (*a*). The same representation of the band structure when a thin layer of n-type segregated dopants is present at the Schottky interface (*b*). Φ_{bn} and Φ_{bp} represent the Schottky barrier to electrons and holes respectively. E_c is the conduction band, E_v is the valence band, E_F is the Fermi level and E_i is the intrinsic Fermi level. Finally, TE corresponds to thermionic emission and FE to field effect.

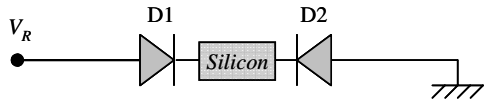

Figure 3. Simplified 1D scheme of the back-to-back structure, where V_R represents the reverse applied voltage and D1 and D2 represent the two opposite Schottky diodes.

Table 1. Characteristics of the different simulated structures.

Structures	Base doping (cm^{-3})	Dopant-segregated layer		$q\Phi_B$ (eV)
		Doping (cm^{-3})	Width (nm)	
NDS1	2×10^{15}	–	–	0.325
DS	2×10^{15}	10^{18}	20	0.325
NDS2	2×10^{15}	–	–	0.254

the equilibrium electron density that directly translates into the concentration of activated dopants follows a law of thermal activation $\sim\exp(-0.47\ eV\ kT^{-1})$ [16]. Considering that As segregation is generally produced at temperatures in the 500–700 °C range [17], it was found reasonable to limit the concentration of activated segregation to 10^{18} cm^{-3}.

The n-type silicon substrate doping ('base' doping) is 2×10^{15} cm^{-3} and the Schottky barrier height 0.325 eV (see table 1). The equivalent surface of the contacts is equal to 4×10^4 μm^2. The length of the simulated device is 2.72 μm. The characteristic transport paths in real back-to-back diodes (typically over 100 μm) would mean unaffordable CPU times from the Monte Carlo point of view. Therefore, a temperature-dependent silicon resistance (e.g. 164 Ω at 300 K) has been properly considered in the Monte Carlo simulation to account for a realistic silicon substrate length. This procedure was successfully applied in previous works [18].

A one-dimensional Monte Carlo simulator (including scattering with impurities, acoustic and optical phonons) self-consistently coupled to a Poisson solver has been used [19] in order to perform the simulations. The study is carried out in the ⟨1 0 0⟩ crystallographic direction. Both thermionic injection (from metal to semiconductor) and absorption (from semiconductor to metal), together with direct quantum tunneling processes, have been incorporated in our model using the WKB approach [15, 20] to solve the Schrödinger

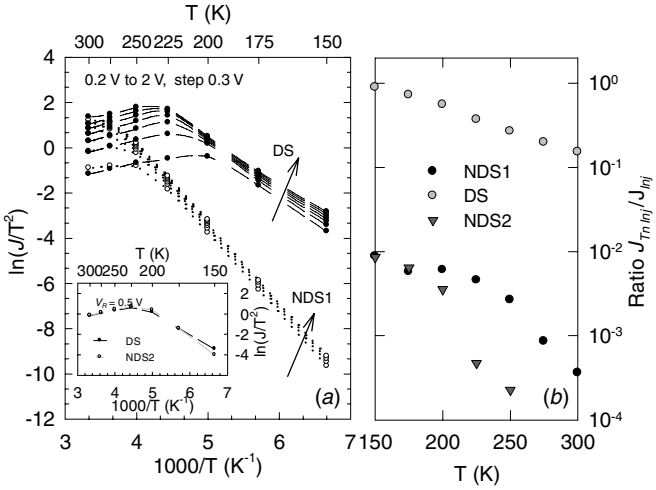

Figure 4. (*a*) Arrhenius plot for the n-type NDS1 and DS back-to-back diode analyzed for several reverse bias applied (from 0.2 V to 2 V, step of 0.3 V). Inset of the figure: Arrhenius plot at $V_R = 0.5$ V for DS and NDS2 back-to-back diodes. (*b*) Ratio between the tunneling injection component and the total injected current for the three structures studied.

equation in the direction perpendicular to the contact. Barrier lowering due to image charge effects is also taken into account (further details are given in [21]). The statistical enhancement technique based on an expansion/compression algorithm has been considered [22] in order to achieve accurate current values in the reverse bias regime.

3. Results and discussion

Figure 4(*a*) shows the comparison (by means of the Arrhenius plot) of the current obtained in the NDS1 and DS structures for several values of reverse applied voltage, V_R (these reverse voltages will be expressed as absolute values). Two different temperature regimes are observed. At low temperatures, the typical exponential decay as a function of T^{-1} predicted by the thermionic emission/diffusion theory is observed [15]. However, at higher temperatures, the Schottky law is not obeyed and a decrease of current is obtained as the temperature increases. This change of behavior is associated with the increase of the silicon resistance and a decrease of the Schottky barrier resistance when the temperature gets augmented [6],

giving rise to the appearance of a maximum in the Arrhenius plot. The location of this maximum corresponds to about 275 K for the NDS1 structure while for the DS back-to-back diode it gets shifted toward lower temperatures (about 225 K) as can be observed in figure 4(*a*). Moreover, the presence of the dopant-segregated layer yields an important increase of current for the DS structure, particularly in the low temperature range. It can therefore be deduced that the effect of the dopant-segregated layer would be comparable to a reduction of the effective Schottky barrier height in a homogenous NDS1 structure. Additional MC simulations show that the total current of a structure with no dopant-segregated layer structure with a barrier height equal to 0.254 eV (NDS2, see table 1) is analogous to the current of the DS one (inset of figure 4(*a*) shows this fact for $V_R = 0.5$ V). For comparison purposes, we will consider and present results for this NDS2 structure also. Even if the effect of the DS layer on the total current is equivalent to a reduction of the effective barrier in the NDS1 structure, the origin of the currents is not the same as is reflected in figure 4(*b*), where the ratio of the tunneling injection current over the total injection current is shown for the three simulated structures. The contribution of the tunneling component to the total injection current is dominant in the low temperature region for the DS structure, while for the NDS1 and NDS2 diodes the tunneling processes are not so important, the thermionic injection being the most relevant contribution to the total current.

A rigorous analysis of carrier transport inside the device is required to completely analyze the effects of introducing a dopant layer close to the Schottky contact. For this task, we will take advantage of the analysis of different internal quantities provided by the Monte Carlo simulator.

We will now proceed to examine the two temperature ranges previously observed in the Arrhenius plot, with the reverse-biased junction dominating the current behavior for low temperatures, and the resistive behavior of the device at high temperatures. Figure 5 shows the conduction band, the electric field and the carrier density profiles for the NDS1 and DS structures at $V_R = 0.5$ V and for several temperatures.

Under low temperature conditions, in the NDS1 diode, a very significant curvature of the conduction band appears (see figure 5) due to the difference between the conduction band and the Fermi level and also for the reverse applied voltage. As a consequence of this curvature, as the carriers are injected into the structure from the reverse-biased junction, they are rapidly accelerated due to the high values of the electric field (see figure 5(*b*), where we observe that at the Schottky junction, the value of the electric field for 175 K is -20 kV cm^{-1}) and move further away from the Schottky interface. This is translated into a wide depletion region (figure 5(*c*)), which is highly resistive and accounts for most of the potential drop from one contact to the other [21], also explaining that the behavior of the structure is properly described by the Schottky law, as was previously mentioned. The effect of the electric field over carriers is better explained by means of the carrier velocity distribution function (VDF), shown in figure 6 for a temperature value into this range (175 K). Close to the contact, the VDF is a positive hemi-Maxwellian that corresponds to

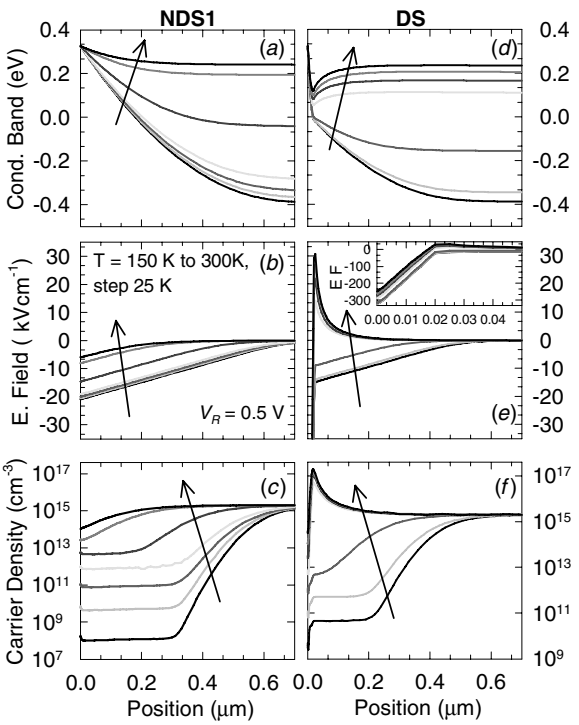

Figure 5. NDS1 back-to-back diode: (*a*) conduction band, (*b*) electric field and (*c*) carrier density as a function of the position at $V_R = 0.5$ V (extrinsic voltage applied to the back-to-back diode; it must be noticed that intrinsic MC voltage tends to reduce as the temperature is raised, in accordance with the increase of the silicon resistance) for several temperatures from 150 K to 300 K. DS back-to-back diode: (*d*) conduction band, (*e*) electric field and (*f*) carrier density under the same bias and temperature conditions. The inset of (*e*) represents a zoom over the first 50 nm of the device; however, in the vertical axis it shows the complete range of values reached by the electric field.

the carriers entering the device, as is portrayed at 0.25 nm (figure 6). When electrons move inside the depletion region, toward the right, two different peaks appear in the VDF, the one at lower velocities corresponds to the carriers in the longitudinal X valleys (whose effective mass is 0.91 m_0) and the faster peak to the carriers in the transversal valleys (lighter than the previous ones, 0.19 m_0). These two peaks are associated with quasiballistic transport, as evidenced by the number of scatterings with phonons undergone by a carrier as a function of the position (figure 7(*a*)), which shows that this number is lower than 1 at the first nanometers away from the reverse-biased contact. Under the action of the strong electric field, the carriers acquire more velocity as they leave the contact behind; this is translated into a scrolling of the ballistic peaks of the VDF to higher velocity values as can be observed in figure 6, at the transition from 5.5 nm to 10.5 nm. However, once the electrons surpass the space-charge region, the number of scatterings rapidly augments and the electric field gets close to zero, thus yielding a quasi-diffusive carrier transport as reflected in the VDF for 225 nm, whose shape approaches a full Maxwellian [21].

However, when a dopant-segregated layer is considered adjacent to the contact, as a consequence of the elevated local doping, the conduction band gets bent in the region close to

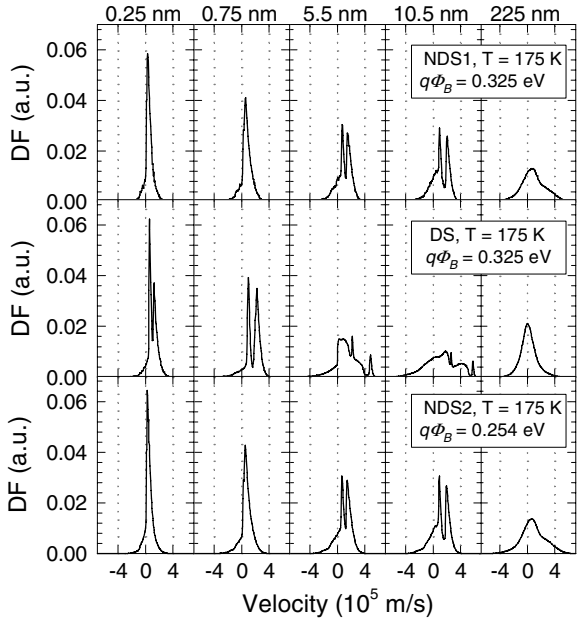

Figure 6. Velocity distribution function for the NDS1 (top), DS (center) and NDS2 (bottom) structures at 175 K for $V_R = 0.5$ V at 0.25 nm, 0.75 nm, 5.5 nm, 10.5 nm and 225 nm from the reverse-biased Schottky contact.

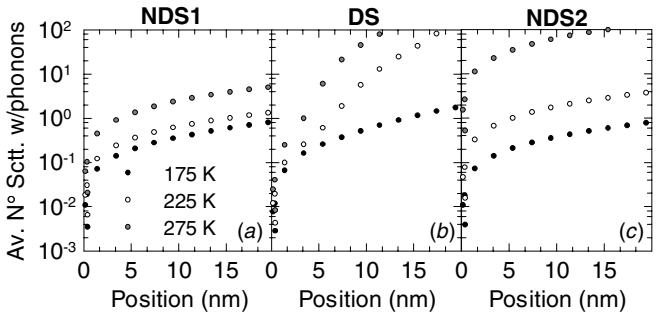

Figure 7. Average number of scattering events suffered in the first 20 nm of the devices for several temperatures at $V_R = 0.5$ V. This magnitude is obtained averaging over time and electron ensemble.

the reverse Schottky contact, yielding a larger slope and a thinner tunneling path (figure 5(*d*)) when compared with the NDS1 structure (figure 5(*a*)); it must also be noticed that the space charge region is also smaller (0.3 μm for the NDS1, figure 5(*c*), and 0.2 μm for the DS structure, figure 5(*f*)). For this reason, as carriers get inside the device they come across an extremely high value of electric field in the first 20 nm of the device (around 320 kV cm^{-1}, see inset of figure 5(*e*)) being much more accelerated than in the NDS1 diode. In this case, the already mentioned ballistic peaks of the VDF are present even at 0.25 nm from the contact and are rapidly shifted toward higher velocities (see VDF at 5.5 nm of the NDS1 structure for comparison). However, the action of the scattering mechanisms is more intense in this case, and the diffusive behavior (wider VDF) is also present. Moreover, still in the low temperature range, when the electrons overcome the DS layer, there is a change of slope in the electric field (see the inset of figure 5(*e*)), indicating that the carriers are still getting accelerated but not in such a strong way as before. The

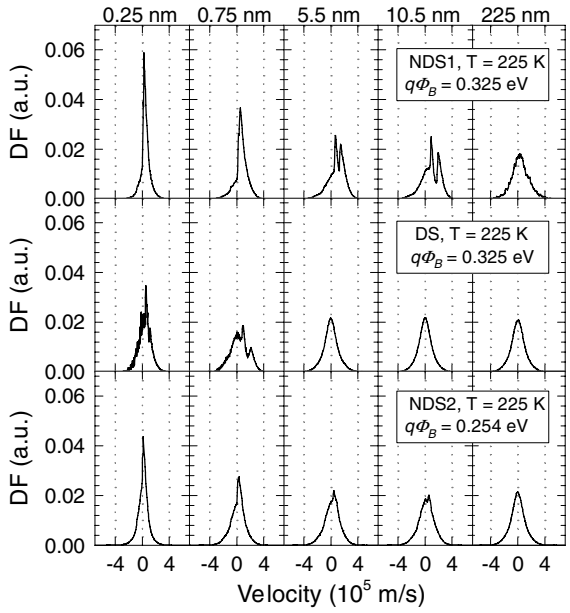

Figure 8. Velocity distribution function for the NDS1 (top), DS (center) and NDS2 (bottom) structures at 225 K for $V_R = 0.5$ V at 0.25 nm, 0.75 nm, 5.5 nm, 10.5 nm and 225 nm from the reverse-biased Schottky contact.

number of scattering mechanisms has rapidly increased as the carriers move away from the contact, and so, those electrons that initially presented a strong ballistic behavior, now portray a strong diffusive transport under the scattering effect, as can be observed in the VDF from 10.5 to 225 nm for the DS structure.

In the case of the NDS2 back-to-back diode, it presents similar behavior to the NDS1 (see table 1). The conduction band, electric field and carrier density profiles present a similar shape to that of the NDS1 structure (not shown in the graphs), so there are not many differences in the VDF. The increase of the current shown previously in figure 4 is due to the favoring of the thermionic injection over the Schottky barrier, because of the lower barrier height.

At higher temperatures (figure 8, 225 K), for the DS (center of the figure) and NDS2 (bottom of the figure) structures, the silicon resistance is dominant as compared to the Schottky barrier one, while the NDS1 structure still follows the Schottky law in the Arrhenius plot. This means that for the NDS1 structure, the circumstances are similar to those at 175 K, but with a lower value of the electric field which results in less prominent peaks of the VDF (see figure 8). However, for the DS structure the conduction band presents a well-formed band with bending induced by the DS layer (see figure 5(*d*)), with the corresponding accumulation of carriers next to the junction (figure 5(*f*)). This fact yields that over the first nanometers from the interface (where the electric field is negative, see figure 5(*e*)), electrons are abruptly accelerated inside the device through the thin energy barrier. However, as soon as the electric field becomes positive, electrons are decelerated. Sufficiently far from the junction, the electric field tends to zero, reaching a quasi-diffusive situation. It is also interesting to evaluate the differences between the DS and NDS2 structures, because of the previously mentioned

change of behavior in the Arrhenius plot. Although the current obtained through the two junctions is the same (inset of figure 3(*a*)), there are some differences related to carrier transport. We observe that at larger temperatures in the DS diode, the two peaks of the VDF relative to the carriers in the longitudinal and transversal valleys still appear close to the junction, while in the NDS2 structure the diffusive VDF profile is rapidly reached. This means that the ballistic transport is enhanced (even for the higher temperatures) with the inclusion of the DS layer. However, as the temperature rises so also does the probability of phonon scattering, which originates a strong momentum relaxation. This fact, combined with the local positive values of the electric field a few nanometers away from the interface, provokes the carriers into showing diffusive transport features in a region closer to the contact than in the case of lower temperatures. As compared to the NDS1 structure, the one including dopant segregation shows a VDF with diffusive features at a distance closer to the contact (5.5 nm).

4. Conclusions

A Monte Carlo analysis of the consequences of including a dopant-segregated layer adjacent to the Schottky contacts of back-to-back diodes has been presented. The effect of the temperature over the total current is evaluated by means of the Arrhenius plot. A strong band bending arises close to the interface, enhancing the tunneling current; it has been proved that the effect over the total current is equivalent to lowering of the effective Schottky barrier height. However, significant differences appear related to carrier transport between the homogeneous structure and the dopant segregated back-to-back. Results have evidenced that although carriers in the NDS1 structure present ballistic features in a wider region than in the DS one, the electrons in the DS back-to-back diode are faster at the vicinity of the contact due to the extremely high values of the electric field originated by the dopant-segregated layer, observing so an augmented contribution of ballistic transport in the first few nanometers from the Schottky interface. In general, the dopant segregation can be considered as a valuable technique to increase carrier injection, promote ballistic transport and achieve lower effective barrier heights in structures like SB-MOSFETS.

Acknowledgments

The authors would like to thank Raphael Valentin from the Institut d'Electronique de Microelectronique et de Nanotechnologie, IEMN in France. This work has been supported by the research project METAMOS (IST-16677) financed by the European Comission and the project SA010A07 from the Consejería de Educación de la Junta de Castilla y León in Spain.

References

[1] *The International Technology Roadmap for Semiconductors, San Jose, CA* 2005 http://public.itrs.net
[2] Lee M L and Fitzgerald E A 2003 *IEDM '03 Technical Digest* p 18.1.1
[3] Ikeda K *et al* 2002 *IEEE Electron Device Lett.* **23** 670
[4] Connelly D, Faulkner C and Grupp D E 2003 *IEEE Trans. Electron Devices* **50** 1340
[5] Connelly D, Faulkner C and Grupp D E 2003 *IEEE Electron Device Lett.* **24** 411
[6] Dubois E and Larrieu G 2004 *J. Appl. Phys.* **96** 729
[7] Kedzierski J *et al* 2000 *IEDM Technical Digest* p 57
[8] Zhu S *et al* 2004 *IEEE Electron Device Lett.* **25** 565
[9] Kinoshita A *et al* 2004 *VLSI Symp. Technical Digest* p 168
[10] Larrieu G *et al* 2007 *International Electron Device Meeting, IEDM'07 (Washington)*
[11] Chen B and Chen M 1996 *IEEE Trans. Electron Devices* **43** 258
[12] Knoch J *et al* 2005 *Appl. Phys. Lett.* 87
[13] Zhang M *et al* 2006 *Solid-State Electron.* **50** 594
[14] Tsui B-Y and Lu C-P 2007 *Conf. Proc. ESSDERC 07* p 307
[15] Sze S M 1981 *Physics of Semiconductor Devices* 2nd edn (New York: Wiley)
[16] Derdour A M, Nobili D and Solmi S 1991 *J. Electrochem. Soc.* **138** 857
[17] Zhang Z, Qiu Z, Liu R, Östling M and Zhang S L 2007 *IEEE Electron Device Lett.* **28** 565
[18] Pascual E, Rengel R, Reckinger N, Tang X, Bayot V, Dubois E and Martín M J 2008 *Phys. Status Solidi* c **5** 119
[19] Martín M J, Velázquez J E and Pardo D 1997 *J. Appl. Phys.* **79** 7975
[20] Rengel R, Pascual E and Martín M J 2007 *IEEE Electron Device Lett.* **28** 171
[21] Pascual E, Rengel R and Martín M J 2007 *Semicond. Sci. Technol.* **22** 1003
[22] Martín M J, González T, Pardo D and Velázquez J E 1996 *Semicond. Sci. Technol.* **11** 380